Cancer Cell
Article

Raf-1 Addiction in Ras-Induced Skin Carcinogenesis

Karin Ehrenreiter,[1] Florian Kern,[1] Vanishree Velamoor,[1] Katrin Meissl,[1] Gergana Galabova-Kovacs,[1] Maria Sibilia,[2] and Manuela Baccarini[1,*]
[1]Max F. Perutz Laboratories, Department of Microbiology and Immunobiology, University of Vienna, 1030 Vienna, Austria
[2]Department of Medicine I, Institute for Cancer Research, Medical University of Vienna, 1090 Vienna, Austria
*Correspondence: manuela.baccarini@univie.ac.at
DOI 10.1016/j.ccr.2009.06.008

SUMMARY

Ras activation is common to many human cancers and promotes cell proliferation and survival by initiating multiple signaling cascades. Accordingly, Ras-transformed cells are generally considered too resourceful to become addicted to a single effector. In contrast to this tenet, we now demonstrate an absolute, cell autonomous requirement for Raf-1 in the development and maintenance of Ras-induced skin epidermis tumors. Mechanistically, Raf-1 functions as an endogenous inhibitor dimming the activity of the Rho-dependent kinase Rok-α in the context of a Ras-induced Raf-1:Rok-α complex. Raf-1-induced Rok-α inhibition allows the phosphorylation of STAT3 and Myc expression and promotes dedifferentiation in Ras-induced tumors. These data link the Raf-1:Rok-α complex to STAT3/Myc activation and delineate a pathway crucial for cell fate decision in Ras-induced tumorigenesis.

INTRODUCTION

The epidermis shields the body from the potentially, or frankly, harmful effects of the environment. Due to the wear and tear to which it is subjected, the epidermis is in a constant state of self-renewal. This process requires the proliferation of basal keratinocytes, which, after detaching from the underlying basement membrane of extracellular matrix, withdraw from the cell cycle and differentiate while migrating toward the skin surface. The disruption of the balance between keratinocyte proliferation and their ability to differentiate and/or to undergo apoptosis causes several pathological conditions, including tumorigenesis. Squamous cell carcinoma (SCC), one of the most common human skin cancers, results from such an imbalance between proliferation, differentiation, and apoptosis (Ridky and Khavari, 2004). The pathways required to convert normal epidermis into SCC are still incompletely defined, but there is strong evidence indicating that activation of Ras signaling concomitant with inhibition of NF-κB function is sufficient to transform normal human epidermis into SCC (Green and Khavari, 2004).

Ras GTPases are activated by a variety of extracellular signals and are mutated in 33% of human cancers. Activated Ras stimulates multiple effectors, including the Raf/MEK/ERK pathway, the phosphoinositide-3 kinases (PI-3K)/Akt pathway, and the guanine nucleotide exchange factors Ral-GDS and Tiam-1, which lead to the activation of the small GTPases Ral and Rac, respectively (Repasky et al., 2004). These different effectors of Ras contribute to distinct aspects of transformation. While the PI-3K pathway (Gupta et al., 2007; Sibilia et al., 2000) and Ral-GDS (Gonzalez-Garcia et al., 2005) have been implicated in cell survival, the ERK pathway has long been regarded as the mitogenic branch of Ras signaling. Deregulation of this pathway has been reported in more than 30% of common cancers. In the specific case of SCC, the majority of spontaneous human tumors display Ras and ERK activation in the absence of somatic Ras mutations, suggesting that other factors, such as the overexpression of receptor tyrosine kinases, may activate the pathway in tumors (Dajee et al., 2003).

Consistent with the mitogenic role attributed to the Ras/ERK pathway, studies in mouse and human epidermal cells in vivo have associated the activation of its components with increased proliferation and decreased differentiation (Dajee et al., 2002; Haase et al., 2001; Scholl et al., 2004; Tarutani et al., 2003), although constitutive Ras/Raf activation can arrest growth and

SIGNIFICANCE

Our data show that Ras-driven carcinogenesis requires the continuous presence of Raf-1 to restrain Rok-α activity and prevent differentiation. Since Raf-1 is dispensable for epidermal homeostasis, this discovery paves the way for the design of molecule-targeted therapies, which may include Raf-1 interference or allosteric inhibitors capable of disrupting the Raf-1:Rok complex. The combination of chemotherapy and induction of tumor cell differentiation (differentiation therapy) has revolutionized the treatment of leukemia. The complete differentiation induced by Raf-1 ablation in vivo provides proof of principle that such differentiation therapy may be applied to solid tumors and raises hopes that a combination of Raf-1-targeted and conventional therapies may be beneficial at least in the treatment of skin epidermis tumors containing active Ras.

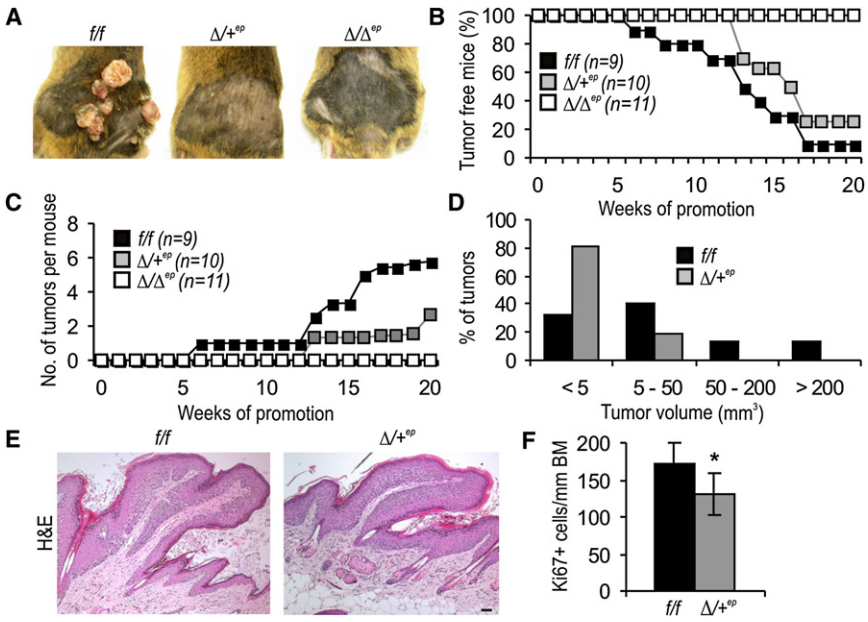

Figure 1. Raf-1 Ablation in Keratinocytes Prevents Chemically Induced Skin Carcinogenesis

Eight- to twelve-week-old *f/f*, $\Delta/+^{ep}$ and Δ/Δ^{ep} mice were subjected to chemical two-stage carcinogenesis with DMBA and TPA.

(A–D) Δ/Δ^{ep} mice are completely resistant and $\Delta/+^{ep}$ mice are partially resistant to chemically-induced skin carcinogenesis. (A) shows representative pictures of *f/f*, $\Delta/+^{ep}$ and Δ/Δ^{ep} animals. (B) shows tumor incidence (C) shows the average number of tumors per mouse. (D) shows tumor size. (E) Lack of major structural differences in $\Delta/+^{ep}$ and *f/f* tumor sections stained with hematoxylin and eosin. The scale bar represents 100 μm.

(F) Mitotic index of *f/f* and $\Delta/+^{ep}$ tumors. Proliferation was determined as the number of Ki67+ cells per millimeter of basal membrane (BM). Three millimeters of BM/mouse were analyzed. The plot shows the results of the analysis of at least three animals/genotype. Error bars indicate SD of the mean. *$p < 0.01$ according to Student's t test.

induce features of terminal differentiation in cultured murine keratinocytes (Lin and Lowe, 2001; Roper et al., 2001). Therefore, the Raf/MEK/ERK arm of Ras signaling represents an attractive target for the therapy of skin cancer. As a caveat to this statement, human tumor cells harboring Ras mutations are quite resistant to the inhibition of MEK (Solit et al., 2006), and while the Raf/MEK/ERK pathway is important in tumor induction, other Ras effectors may be more relevant for the maintenance of established tumors, at least in a xenograft model (Lim and Counter, 2005).

Rho family GTPases have also been implicated in the control of keratinocyte proliferation and differentiation, in the context of both epidermal homeostasis and tumor development (Benitah et al., 2005; Grossi et al., 2005; Lefort et al., 2007; Malliri et al., 2002; Wu et al., 2006). Particularly, RhoA effectors have been reported to both promote (McMullan et al., 2003) and antagonize (Grossi et al., 2005; Lefort et al., 2007) keratinocyte differentiation.

Well-characterized transgenic and chemical models of skin carcinogenesis are available in which both the onset and progression of tumors can be readily monitored. Recently, we have generated a transgenic mouse model in which constitutive activation of the endogenous Ras pathway is achieved by the expression of a dominant active Son of Sevenless (SOS) in the epidermis (*K5-SOS-F* transgenic mice; Sibilia et al., 2000). In the presence of a functional EGFR, required to provide an essential survival signal to tumor cells, *K5-SOS-F* mice develop skin tumors that share features of human SCC (Sibilia et al., 2000).

In the classical chemical carcinogenesis protocol, tumors are initiated by the topical application of 7,12-dimethylbenz[*a*] anthracene (DMBA), which causes a mutation in codon 61 of the H-*ras* gene (Quintanilla et al., 1986), and promoted by the repeated application of 12-O-tetradecanoylphorbol 13-acetate (TPA). The development of these chemically induced tumors critically depends on inflammation (Mueller, 2006) and is reduced to various degrees by the ablation of H-Ras (Ise et al., 2000), of the Rac GEF Tiam-1 (Malliri et al., 2002), and of RalGDS (Gonzalez-Garcia et al., 2005) in the whole animal. Whether the effects of Tiam1 or RalGDS ablation on carcinogenesis reflect the interruption of Ras signaling in the tumor target cell, or defects in accessory cells (inflammatory cells and tumor-associated fibroblasts) or a combination of both, remains to be conclusively established. We have generated an epidermis-restricted Raf-1 knockout (*K5-Cre;c-raf-1*$^{flox/flox}$ mice; hereafter referred to as Δ/Δ^{ep} [Ehrenreiter et al., 2005]), which enables us to investigate the function of Raf-1 in keratinocytes during skin carcinogenesis. Δ/Δ^{ep} animals develop normally, except for a mild waved fur phenotype that disappears after the first hair cycle and a significant delay in repairing full-thickness wounds, which correlates with a migratory defect of the keratinocytes. The molecular basis of this defect is the hyperactivity of the Rho effector Rok-α, whose activation in wild-type cells is inhibited by Raf-1 in a kinase-independent manner. In contrast, activation of ERK is not affected by Raf-1 ablation (Ehrenreiter et al., 2005). Here, we use the Δ/Δ^{ep} animals as well as a mouse strain allowing tamoxifen-inducible, epidermis-restricted Raf-1 ablation (Indra et al., 1999) to investigate the role of Raf-1 in Ras-driven epidermis carcinogenesis.

RESULTS

Raf-1 Ablation Prevents Ras-Dependent Tumor Formation

We assessed the role of Raf-1 in Ras-dependent tumor formation by combining epidermis-restricted Raf-1 ablation (Δ^{ep}, deleted in epidermis [Ehrenreiter et al., 2005]) with the DMBA/TPA chemical carcinogenesis protocol. In wild-type (*f/f*) mice, this protocol resulted in the development of visible tumors within 6 weeks of application of DMBA/TPA on dorsal skin, with a 50% penetrance by week 13. In heterozygous ($\Delta/+^{ep}$) littermates tumor development was severely retarded, starting at week 13 and reaching an incidence of 50% by week 17 (Figure 1B). In addition, the average number of tumors/mouse was significantly reduced in the $\Delta/+^{ep}$ group (two to three tumors/mouse compared with

five to six tumors/mouse in the wild-type cohort; Figures 1A and 1C). The $\Delta/+^{ep}$ tumors were much smaller than the *f/f* tumors and most of them did not reach a volume of >5 mm^3 at week 20 (Figures 1A and 1D). Tumor development was completely blocked in homozygous Δ/Δ^{ep} mice (Figures 1A and 1B). Histological examination at week 20 did not reveal any major differences in *f/f* and $\Delta/+^{ep}$ tumors of similar size, all of which were papillomas with a clear cut border, projecting above the surrounding tissue (Figure 1E). The numbers of proliferating Ki67+ cells were slightly but significantly reduced in $\Delta/+^{ep}$ tumors (Figure 1F). Few apoptotic cells could be visualized by TUNEL staining and their numbers were indistinguishable in *f/f* and $\Delta/+^{ep}$ tumors of the same size (see Figure S4A available online). Thus, Raf-1 gene dosage is a critical determinant in DMBA-induced tumor initiation, as shown by the reduced numbers and delayed appearance of tumors in the heterozygotes, and contributes to TPA-induced tumor promotion, as reflected by the decreased proliferative index observed in $\Delta/+^{ep}$ tumors.

Typically, DMBA induces tumor initiation by causing an activating mutation in codon 61 of the *ras* gene (Quintanilla et al., 1986). Therefore, the data above strongly suggest a requirement for Raf-1 in Ras-driven skin tumorigenesis. In the majority of human SCCs, however, endogenous Ras signaling is activated in the absence of such activating mutations (Dajee et al., 2003). To mimic this condition, we used a genetic model in which an activated form of the Ras-GEF SOS is expressed under the control of the K5 promoter in basal keratinocytes and in the outer root sheath of the hair follicles, resulting in the synchronous formation of fast-growing tumors, mostly papillomas (Sibilia et al., 2000). These tumors grow predominantly on the tail, behind the ears, and at sites subjected to scratching and biting. This distribution has also been observed in transgenic animals expressing activated Ha-Ras from a keratin 10 (K10) promoter and suggests that minor injuries promote tumor development (Bailleul et al., 1990). In the 129 genetic background, 100% of *f/f* and $\Delta/+^{ep}$ mice developed visible tumors by the first and second month of life, respectively (Figure 2A). As already noted for the chemical carcinogenesis protocol, $\Delta/+^{ep}$ tumors were much smaller than those arising in *f/f* mice (Figure 2B). The Δ/Δ^{ep} mice did not develop any tumors until 6 months of age (Figure 2A); thereafter, visible tumors started growing very slowly in 20% of the mice. These tumors were identified as escapers in which Raf-1 deletion was incomplete and were not analyzed further (Figure S1).

We next analyzed small, medium, and large *f/f* and $\Delta/+^{ep}$ tumors (from 0.3–1.2 cm diameter). The gross histological appearance of size-matched tumors was similar (Figure 2C); however, the cells in the $\Delta/+^{ep}$ lesions were smaller in size than *f/f* tumor cells and showed a higher degree of compaction (Figure 2C). Loss of an orderly basal layer, keratin pearls, and clusters or strands of $K5^+$ tumor cells in the dermis, as well as microinvasions, were observed in the large *f/f* (Figures 2C, 2D, and 3D) and occasionally in the $\Delta/+^{ep}$ lesions (data not shown). $\Delta/+^{ep}$ tumors featured less $BrdU^+$ proliferating cells, which were confined to the basal layer (Figure 2E and data not shown). In addition, whereas $\leq$25% of the cells in wild-type tumors expressed the differentiation marker K10 (Grade 3–4 according to Broder's classification), $\Delta/+^{ep}$ papillomas contained around $\geq$75% $K10^+$ cells (Grade 1; Figure 2F). Conversely, the expression of integrin β1, enriched in epidermal stem cells and correlated with the inhibition of keratinocyte differentiation (Levy et al., 2000), was strongly increased in basal and suprabasal cells in *f/f* tumors, but much less so in $\Delta/+^{ep}$ papillomas (Figure 2G). *K5-SOS-F;*Δ/Δ^{ep} epidermis contained only sporadic integrin β1+ cells. An increase in well-differentiated tumors could also be observed in the DMBA/TPA model (5% of wild-type tumors were well differentiated versus 36% $\Delta/+^{ep}$ papillomas; Figure S2A). The number of apoptotic cells was very low and indistinguishable in *f/f* and $\Delta/+^{ep}$ *K5-SOS-F*+ tumors (Figure S4B).

Raf-1 Is Necessary for the Maintenance of *K5-SOS-F*-Induced Tumors

To determine whether Raf-1 was required for the maintenance of the SOS-F-induced tumors, we used *K5-SOS-F;K5-Cre-ER(T);c-raf-1*$^{f/f}$ mice, which express the Cre recombinase as a fusion protein with the mutated ligand-binding domain of the human estrogen receptor (ER). Binding to 4-hydroxy-tamoxifen (TX), but not to estradiol, stimulates Cre activity (Indra et al., 1999). To induce *c-raf-1* ablation, we injected tumor-bearing *K5-SOS-F;K5-Cre-ER(T);c-raf-1*$^{f/f}$ and their *K5-SOS-F;c-raf-1*$^{f/f}$ littermates with TX (1 mg/day intraperitoneally, five consecutive injections). At the time of injection (P26–P41), the diameter of the lesions was between 0.5 and 0.75 cm. *f/f* tumors continued to grow and doubled or even tripled their size within 2 weeks from the last TX injection. In contrast, the lesions from conditional knockout mice ($\Delta/\Delta^{ep}TX$) decreased in size and became covered in white squames (Figures 3A and 3B), which eventually disappeared (by week 7–8). Most lesions resolved completely and never recurred throughout the life span of the animals. In some cases, the bulk of the tumor was dramatically reduced, but persisting small lesions became evident by week 6 (Figure S3A). The *f/f* allele was not completely converted to Δ/Δ in these lesions, indicating that their persistence was due to incomplete recombination (Figure S3B). Importantly, tumor regression was not observed in mice harboring *K5-SOS-F;K5-Cre-ER(T)* (B.M. Lichtenberger and M.S., unpublished data). The regression of the $\Delta/\Delta^{ep}TX$ tumors was accompanied by an increase in cell compaction and tissue stratification (Figure 3D) and by a striking decrease in the number of proliferating and integrin β1+ cells (Figures 3C and 3E), which became absolutely restricted to the basal level (Figure 3E and data not shown). Conversely, suprabasal K10 staining was restored to the $\Delta/\Delta^{ep}TX$ tumors (Figure 3F). The regressing tumors contained hardly any apoptotic cells (Figure S4C). Together, the data indicate that the regression of Raf-1 knockout tumors is due to a massive increase in the terminal differentiation of the tumor cells (Figure 3F), ultimately shed by the epidermis as squames, which, in combination with the sharp decrease in cell proliferation (Figure 3C), results in net cell loss.

Raf-1 Ablation Promotes the Differentiation of *K5-SOS-F*+ Keratinocytes In Vitro

The increased differentiation induced by the chronic or acute ablation of Raf-1 in tumors could be a default program entered by cells with a reduced proliferative ability; alternatively, an intrinsic propensity of the cells to differentiate could bring about the decrease in proliferation. To discriminate between these two possibilities, we isolated primary keratinocytes from *K5-SOS-F*+ and *K5-SOS-F*− mice to test their ability to proliferate and

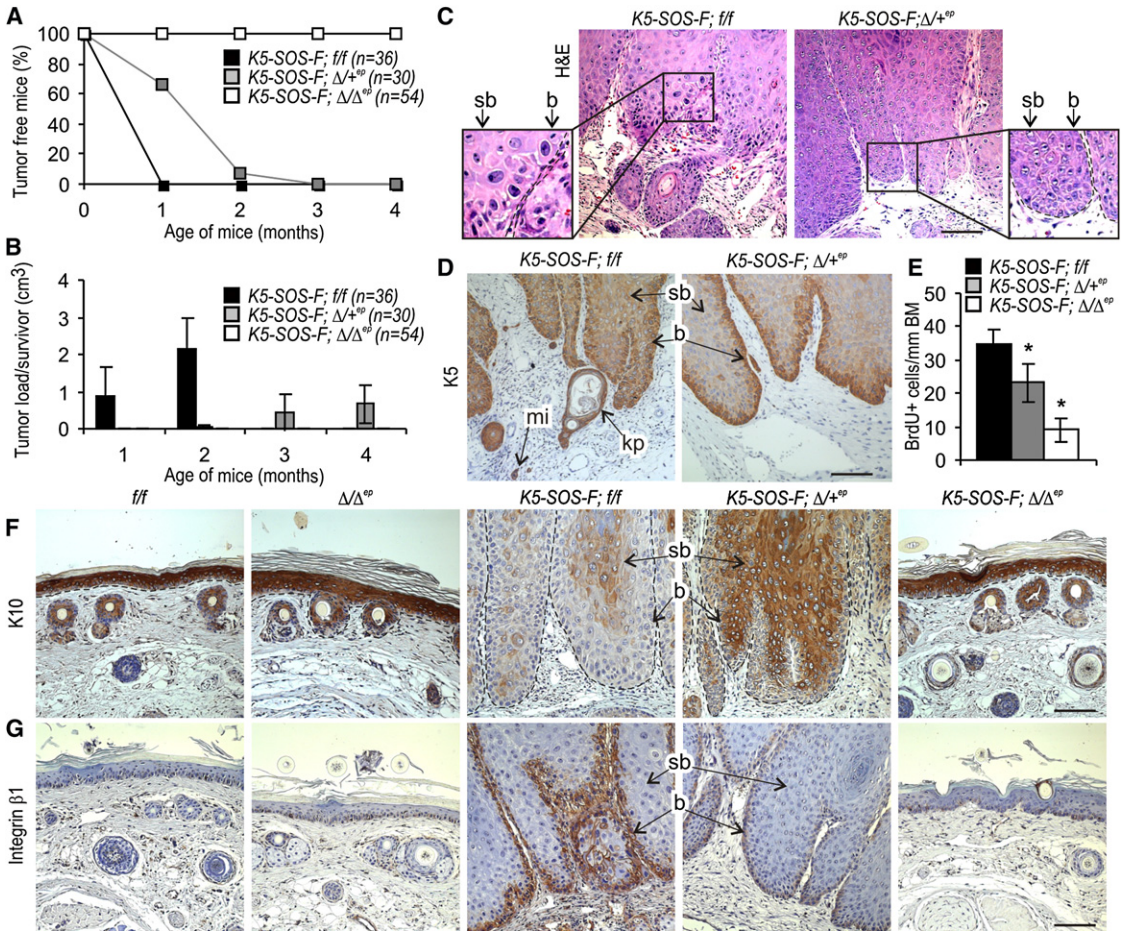

Figure 2. Raf-1 Ablation in Keratinocytes Prevents Tumor Formation and Tumor Progression in *K5-SOS-F*+ Mice

(A and B) Tumor incidence and load in *K5-SOS-F;f/f*, *K5-SOS-F;Δ/+^{ep}* and *K5-SOS-F;Δ/Δ^{ep}* animals.

(C and D) Histochemical and immunohistochemical analysis of size-matched *f/f* and *Δ/+^{ep}* tumor sections stained with hematoxylin and eosin or with a K5 antibody for the basal layer visualization.

(E) Decreased mitotic index (BrdU+ cells/mm BM) in *K5-SOS-F;Δ/+^{ep}* versus *f/f* tumors. The mitotic index of *K5-SOS-F;Δ/Δ^{ep}* epidermis is indistinguishable from that of *f/f* epidermis and is shown as a reference. The plot shows the results of the analysis of at least three animals/genotype.

(F and G) Increased differentiation in *K5-SOS-F;Δ/+^{ep}* compared to *K5-SOS-F;f/f* tumors. Differentiation is shown as K10 positive layers (F). Undifferentiated integrin β1+ cells in *K5-SOS-F;Δ/+^{ep}* are reduced in number and confined to the basal layer compared to *K5-SOS-F;f/f* tumor sections (G). *K5-SOS-F;Δ/Δ^{ep}* epidermis is indistinguishable from that of *f/f* or *Δ/Δ* epidermis. Positive cells are stained in brown. The scale bar represents 100 μm. b, basal layer; sb, suprabasal layer; mi, microinvasions; kp, keratin pearls. The dashed line indicates the border between epidermis and dermis. Error bars indicate SD of the mean. *$p < 0.01$ according to Student's t test.

differentiate in vitro. To avoid measuring a combination of effects on proliferation, differentiation, and apoptosis, the impact of Raf-1 ablation on the proliferative ability of keratinocytes in vitro was determined by assessing the percentage of cells incorporating BrdU. Only few *K5-SOS-F*+ keratinocytes, *f/f* or *Δ/Δ^{ep}* of the 129/Sv background, proliferated in complete media (Figure 4A), possibly because of oncogenic stress, which induces growth arrest in premalignant cells (Collado et al., 2005). Raf-1 ablation had no effect on the percentage of proliferating keratinocytes cultured in complete media (Figure 4A), which was reduced by chemical inhibition of the ERK but not of the Rok pathway (Figure 4A). We next induced keratinocyte differentiation by exposing cells of different genotypes to high concentrations of $CaCl_2$, a method widely used to recapitulate the biochemical events accompanying the transition from the basal to the upper epidermal layers during differentiation in vivo. Differentiation was measured as the number of involucrin+ cells developing in the presence of 1.2 mM $CaCl_2$ (Figures 4B and 4C). *f/f* and *Δ/Δ^{ep}* keratinocytes differentiated efficiently under these conditions, whereas *K5-SOS-F*+;*f/f* keratinocytes failed to do so (Figure 4C; Sibilia et al., 2000). In contrast, *K5-SOS-F* expression did not prevent differentiation of Raf-1-deficient keratinocytes (Figure 4C). Thus, Raf-1 ablation counteracts the *K5-SOS-F*-mediated differentiation block in vivo and in vitro.

Raf-1 Is Required to Restrain Rok Signaling in *K5-SOS-F*+ Cells and Epidermis

To gain insight into the mechanisms underlying the increased differentiation of *K5-SOS-F+;Δ/Δ^{ep}* cells, we monitored the activation of two signaling pathways connected to Ras/Raf and

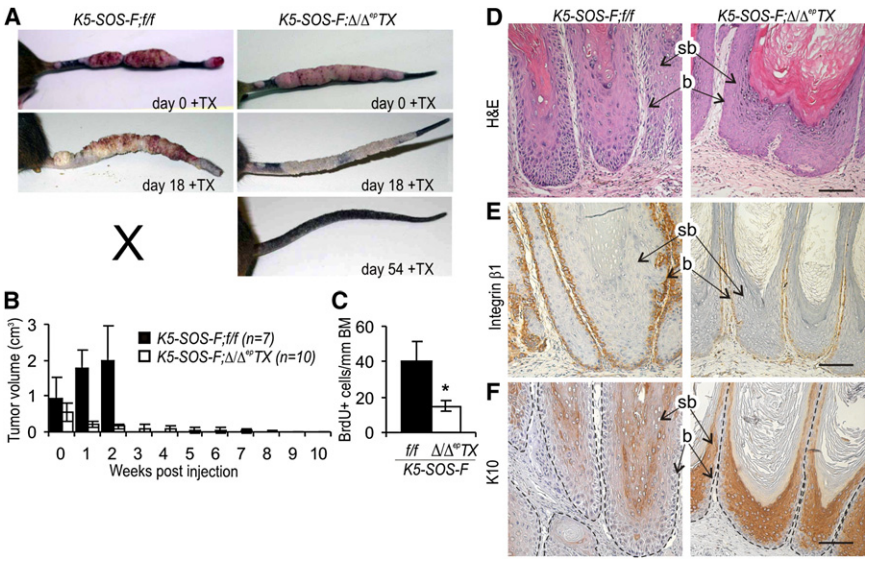

Figure 3. K5-SOS-F Tumors Are Addicted to Raf-1

Tumor-bearing *K5-SOS-F;Δ/Δ^{ep}TX* mice and *K5-SOS-F;f/f* were injected with tamoxifen for five consecutive days and tumor regression was monitored.

(A) Representative pictures of a *K5-SOS-F;f/f* and *K5-SOS-F;Δ/Δ^{ep}TX* mouse after tamoxifen treatment. Note the thick layer of squames on the surface of the regressing tumor. (X) Control mice had to be culled because of the increasing tumor load.

(B) Quantification of tumor regression.

(C) Decreased cell proliferation (BrdU+ cells/mm of BM) in *K5-SOS-F;Δ/Δ^{ep}TX* tumors 7 days after tamoxifen injection. Error bars indicate SD of the mean. *$p < 0.01$ according to Student's t test.

(D–F) Sections of *K5-SOS-F; f/f* and of *Δ/Δ^{ep}TX* tumors 7 days after tamoxifen injection. Note the thick layer of squames in the regressing tumors. (D) shows hematoxylin and eosin staining. Note the increased cell and tissue compaction in *K5-SOS-F;Δ/Δ^{ep}TX* tumors. (E) shows decreased numbers of integrin β1+ cells, and (F) shows increased differentiation (K10 expression) in *K5-SOS-F;Δ/Δ^{ep}TX* tumors compared to *K5-SOS-F;f/f* tumors. Positive cells are stained in brown. The scale bar represents 100 μm.

implicated in keratinocyte differentiation, namely ERK (Schmidt et al., 2000; Wakamatsu et al., 2007) and Rok (McMullan et al., 2003; Vaezi et al., 2002). Treatment of differentiating keratinocytes with chemical inhibitors of these pathways efficiently blocked differentiation of cells of all four genotypes (Figure 4C). Rok inhibition concomitantly increased proliferation in differentiating cultures, whereas MEK/ERK inhibition completely abrogated it (Figure 4D). Both pathways were activated during differentiation: ERK phosphorylation, however, increased only slightly and was essentially indistinguishable in *f/f* and *Δ/Δ^{ep}* cells (Figure 4E, left panel). *K5-SOS-F* expression resulted in a strong increase in ERK phosphorylation that was not affected by the lack of Raf-1 (Figure 4E, right panel). Activation of the Rok pathway was measured by the phosphorylation of the downstream targets myosin light chain 2 (MLC2) and cofilin. MLC2 phosphorylation is required for actin/myosin motor activation and enhances cell contractility (Zhao and Manser, 2005); cofilin is an actin-severing protein whose phosphorylation, mediated by the Rok effector LIMK, promotes actin polymerization. Cofilin phosphorylation increases during the differentiation of cultured human keratinocytes and has been implicated in the compaction of the granular layer of human epidermis in organotypic cultures (Honma et al., 2006). Phosphorylation of MLC2 and (more slightly) of cofilin increased during differentiation of wild-type and Raf-1-deficient keratinocytes, in which it was already present before the induction of differentiation (Figure 4E, left panel). *K5-SOS-F* expression suppressed phosphorylation, particularly of cofilin, but suppression was less severe in *Δ/Δ^{ep}* keratinocytes (Figure 4E, right panel). In addition, consistent with previous reports on the negative regulation of Rok by ERK (Mavria et al., 2006), the phosphorylation of Rok downstream targets was increased by treating the cells with a MEK/ERK inhibitor. In contrast, the Rok inhibitor reduced the phosphorylation of MLC2 and cofilin without affecting ERK phosphorylation (Figure 4E).

Thus, the increased differentiation of Raf-1-deficient keratinocytes in vitro was paralleled by the activation of Rok downstream targets, but not of the ERK pathway. To investigate whether this was the case in vivo, we performed immunohistochemistry on tumor sections from *K5-SOS-F+ f/f*, *Δ/+^{ep}* or *Δ/Δ^{ep}* mice. We found that ERK activation was if anything increased in *Δ/+^{ep}* tumors and in the lesions regressing after Raf-1 ablation. In both cases, phospho-ERK was localized mainly in the terminally differentiating cells of the suprabasal layers, in contrast to the *f/f* tumors in which phospho-ERK staining was observed in the basal layer (Figures 5A and 5B). The pattern of ERK phosphorylation in *K5-SOS-F;Δ/Δ^{ep}* epidermis was indistinguishable from that of *f/f* or *Δ/Δ^{ep}* epidermis not expressing the *K5-SOS-F* transgene (Figure 5A).

In contrast to ERK, cofilin phosphorylation was clearly suppressed in the *f/f* tumors compared to *Δ/+^{ep}* tumors and to *K5-SOS-F;Δ/Δ^{ep}* epidermis (Figure 5C). A similar increase in cofilin phosphorylation was noted in *Δ/+^{ep}* tumors induced by DMBA/TPA (Figure S2B). More importantly, cofilin phosphorylation was strongly induced in the regressing *Δ/Δ^{ep}TX* tumors, concomitantly with the cell compaction and with the massive differentiation caused by Raf-1 ablation (Figure 5D). These results indicate that the expression of the *K5-SOS-F* transgene restrains Rok signaling in keratinocytes in culture and in the epidermis and that *K5-SOS-F*-mediated Rok inhibition is disabled by chronic as well as acute Raf-1 ablation.

Raf-1 physically interacts with Rok-α (Ehrenreiter et al., 2005). To monitor whether K5-SOS-F increased Raf-1:Rok-α interaction in vivo, we prepared crude epidermal lysates and monitored complex formation by assessing the presence of Raf-1 in endogenous Rok-α immunoprecipitates. The crude *Δ/Δ^{ep}* lysates contained a residual Raf-1 band (Figure 5E, left panel), which was absent in pure keratinocyte cultures (Figure 4E) and therefore results from contamination by other tissues, most likely dermis

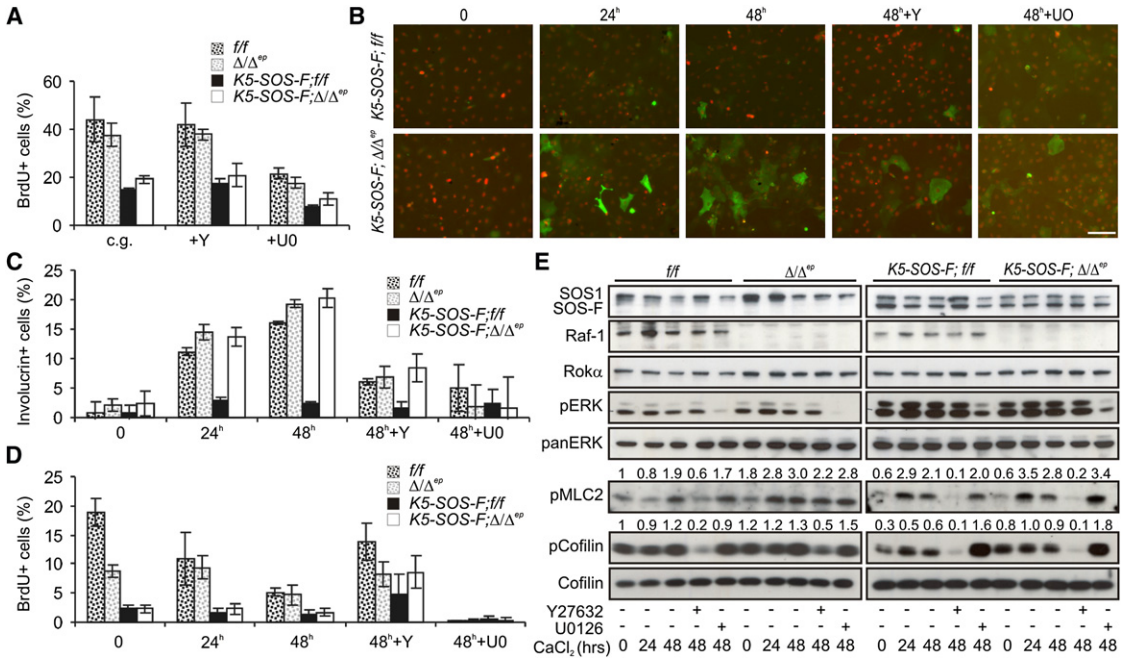

Figure 4. Raf-1 Ablation Enforces the Differentiation of *K5-SOS-F+* Keratinocytes by a Mechanism Involving Rok Activation

(A) Proliferation of primary keratinocytes isolated from *f/f*, *Δ/Δ^{ep}*, *K5-SOS-F;f/f*, and *K5-SOS-F;Δ/Δ^{ep}* mice. Cells of all genotypes were cultured in complete growth medium (c.g., continuously growing). Y-27632 (10 μM) or U0126 (10 μM) were added for inhibition of the Rok and the MEK/ERK pathway, respectively. The percentage of proliferating cells was determined by BrdU incorporation.

(B–D) Raf-1 ablation promotes the differentiation of *K5-SOS-F+* keratinocytes. The percentage of differentiating or proliferating keratinocytes was determined in cultures exposed to 1.2 mM $CaCl_2$ for the indicated time periods in the absence and presence of the inhibitors Y-27632 and U0126. Differentiating cells were defined by the expression of involucrin+ (B and C; green; the scale bar represents 100 μm) and proliferating cells by BrdU+ incorporation (D). The plots in (A), (C), and (D) show a quantification of the results obtained in three different experiments. Error bars indicate SD of the mean.

(E) Increased Rok pathway, but not ERK activation, in *Δ/Δ^{ep}* keratinocytes. Immunoblot analysis of lysates prepared from keratinocytes differentiating in the presence or absence of the Rok or of the MEK/ERK inhibitor is shown. The figures on top of the pMLC2 and pCofilin panels represent a quantification of the intensity of the bands, normalized to loading controls. The value corresponding to wild-type keratinocytes at time point 0 was arbitrarily defined as 1.

and vessels. In *K5-SOS-F+;f/f* lysates, the Raf-1 band was stronger and showed a slower migration that has been correlated with Raf-1 phosphorylation and activation (Figure 5E, left panel). Since the *K5-SOS-F+;f/f* mice already bore tumors of different sizes, the data indicate that Raf-1 increased in tumors, in line with previous observations in human SCC (Riva et al., 1995; Leicht et al., 2007), and that SOS-F expression drove Raf-1 hyperphosphorylation. A Raf-1:Rok-α complex was detectable only in *K5-SOS-F+;f/f* lysates, and its amount was proportional to Raf-1 expression and to the size of the tumor affecting the epidermis (Figure 5E, right panel). Importantly, Rok-α kinase activity was significantly higher in crude lysates of *K5-SOS-F+;Δ/Δ^{ep}* epidermis than in *K5-SOS-F+;f/f* lysates (Figure 5F).

Together, the data indicate that inhibition of Rok signaling by Raf-1 is one of the strategies by which SOS and active Ras inhibit keratinocyte differentiation.

Raf-1 Is Required for STAT3 Activation and Myc Expression in *K5-SOS-F* Tumors

Besides its effects on the actin cytoskeleton, active (unphosphorylated) cofilin enhances the phosphorylation of the transcription factor STAT3 and the expression of its target gene c-*myc* in human psoriatic epidermis (Honma et al., 2006). This mechanism had never been associated with tumorigenesis. Both STAT3 phosphorylation and Myc expression, however, are increased in human SCC (Chen et al., 2008; Seethala et al., 2008; Watt et al., 2008) and promote the development of epidermal hyperplasia and/or malignant tumors in mice (Chan et al., 2007, 2004; Sano et al., 1999; Watt et al., 2008). Therefore, we next determined whether Raf-1 ablation had an impact on STAT3 phosphorylation and Myc expression. pSTAT3+ and Myc+ cells were present at very low levels in *f/f* and *Δ/+^{ep}* epidermis (data not shown) and in *K5-SOS-F+;Δ/Δ^{ep}* epidermis, in which they were essentially confined to the basal layer (Figure 6). A substantial increase in pSTAT3+ and Myc+ cells was detectable in the basal and suprabasal layers of *K5-SOS-F;f/f* and *Δ/+^{ep}* tumors, although the number of pSTAT3+ and Myc+ cells remained significantly lower in the latter (Figure 6A). More importantly, acute ablation of Raf-1 in established tumors caused a dramatic decrease in both STAT3 phosphorylation and Myc expression, and suprabasal staining was no longer observed (Figure 6B).

Topical Application of a Rok Inhibitor Induces Proliferation and Dedifferentiation in *K5-SOS-F;Δ/Δ^{ep}* Epidermis

The data above indicate that Raf-1 ablation limits cofilin activation, STAT3 phosphorylation, and Myc expression during

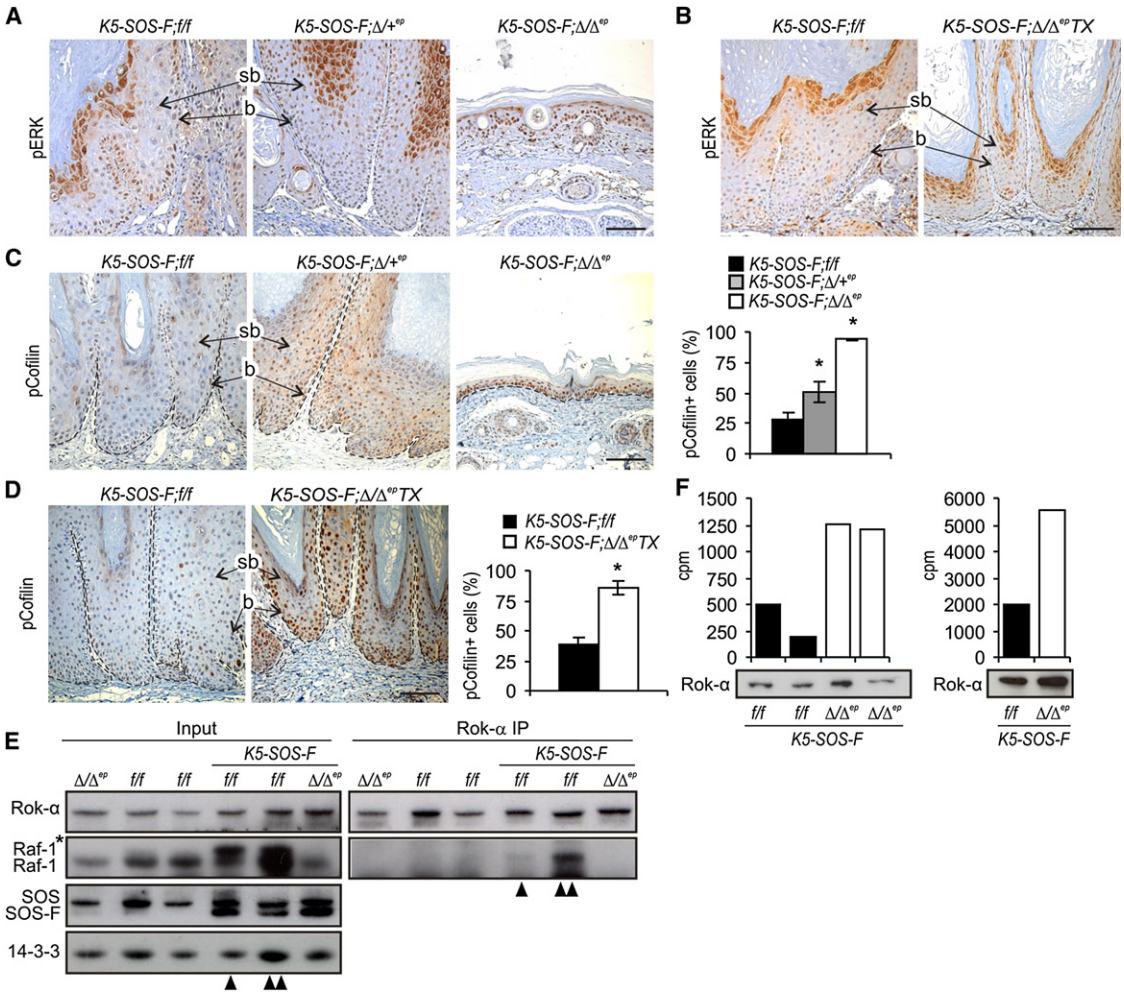

Figure 5. Chronic and Acute Raf-1 Ablation Induces the Phosphorylation of the Rok Downstream Target Cofilin in *K5-SOS-F* Tumors

(A and B) Raf-1 ablation does not affect ERK phosphorylation in *K5-SOS-F* tumors.

(C) Raf-1 ablation increases the phosphorylation (and inactivation) of cofilin in *K5-SOS-F;Δ/+^{ep}* versus *K5-SOS-F;f/f* tumors. *K5-SOS-F;Δ/Δ^{ep}* epidermis is indistinguishable from that of *f/f* or *Δ/Δ^{ep}* epidermis not expressing the *K5-SOS-F* transgene and is shown as a reference.

(D) Regressing *K5-SOS-F;Δ/Δ^{ep}TX* tumors contain high amounts of pCofilin+ cells (day 7 after tamoxifen treatment). ERK and cofilin phosphorylation were determined by immunohistochemistry of skin and tumor sections of the different genotypes as indicated. Positive cells are stained in brown. The scale bar represents 100 μm. The plots represent the results of the analysis of at least three animals/genotype, evaluating ≥600 cells/mouse.

(E) Raf-1 interacts with Rok-α in *K5-SOS-F+* epidermis. Rok-α was immunoprecipitated from crude epidermis lysates. The presence of Raf-1 and Rok-α was detected by immunoblotting in whole-cell lysates (Input) and Rok-α immunoprecipitates (IP). In addition, SOS and SOS-F expression were determined in the crude lysates. 14-3-3 is shown as a loading control. Note that in *K5-SOS-F+* lysates Raf-1 is present as a doublet; the slower migrating form is associated with phosphorylation and possibly activation. The Raf-1 band in the Δ/Δ^{ep} lysates is probably due to contamination by other tissues (dermis or vessels). Arrowheads denote tumor-bearing mice. Tumor volume: 6, 98 mm^3; 66, 236 mm^3. Control tail volume: 78.5 mm^3.

(F) Increased Rok-α activity in crude lysates of *K-SOS-F;Δ/Δ^{ep}* epidermis. The kinase activity of Rok-α immunoprecipitates from 200 μg (left panel) or 400 μg of crude epidermis lysates from *K-SOS-F+ f/f* or *Δ/Δ^{ep}* mice was assessed using the long S6 peptide as a substrate. The amount of Rok-α in the immunoprecipitates is shown below the graphs. Error bars indicate SD of the mean. *p < 0.01 according to Student's t test.

Ras-induced tumor development. This is probably due to Rok-α hyperactivation. To determine whether Rok-α hyperactivation limits activation of the cofilin/STAT3/Myc pathway and tumor development in vivo, we applied the Rok inhibitor Y-27632 on the right ear of *K5-SOS-F;Δ/+^{ep}* or *K5-SOS-F;Δ/Δ^{ep}* mice. The left ear was treated with DMSO as a vehicle and as skin permeation enhancer. We chose the ears for this treatment because the epidermis is thinner than that of other body sites (Porter et al., 1998). A thinner epidermis increases the chances of the inhibitor to reach the basal layer and therefore the target cells. DMSO itself caused skin irritation and some proliferation (3- to 4-fold increase) of the epidermis, as previously described (Lashmar et al., 1989). Y-27632, however, induced a significant increase in the proliferation of *K5-SOS-F;Δ/+^{ep}* and *K5-SOS-F;Δ/Δ^{ep}* epidermis (Figure 7A), measured both as epidermal thickness and as a percentage of BrdU+ cells. Conversely, differentiation, defined by the percentage of K10+ epidermal layers, was strongly reduced (Figure 7B). The inhibitor also caused a reduction in the percentage of pCofilin+ cells as well as a decrease in the intensity of pCofilin staining. The latter aspect

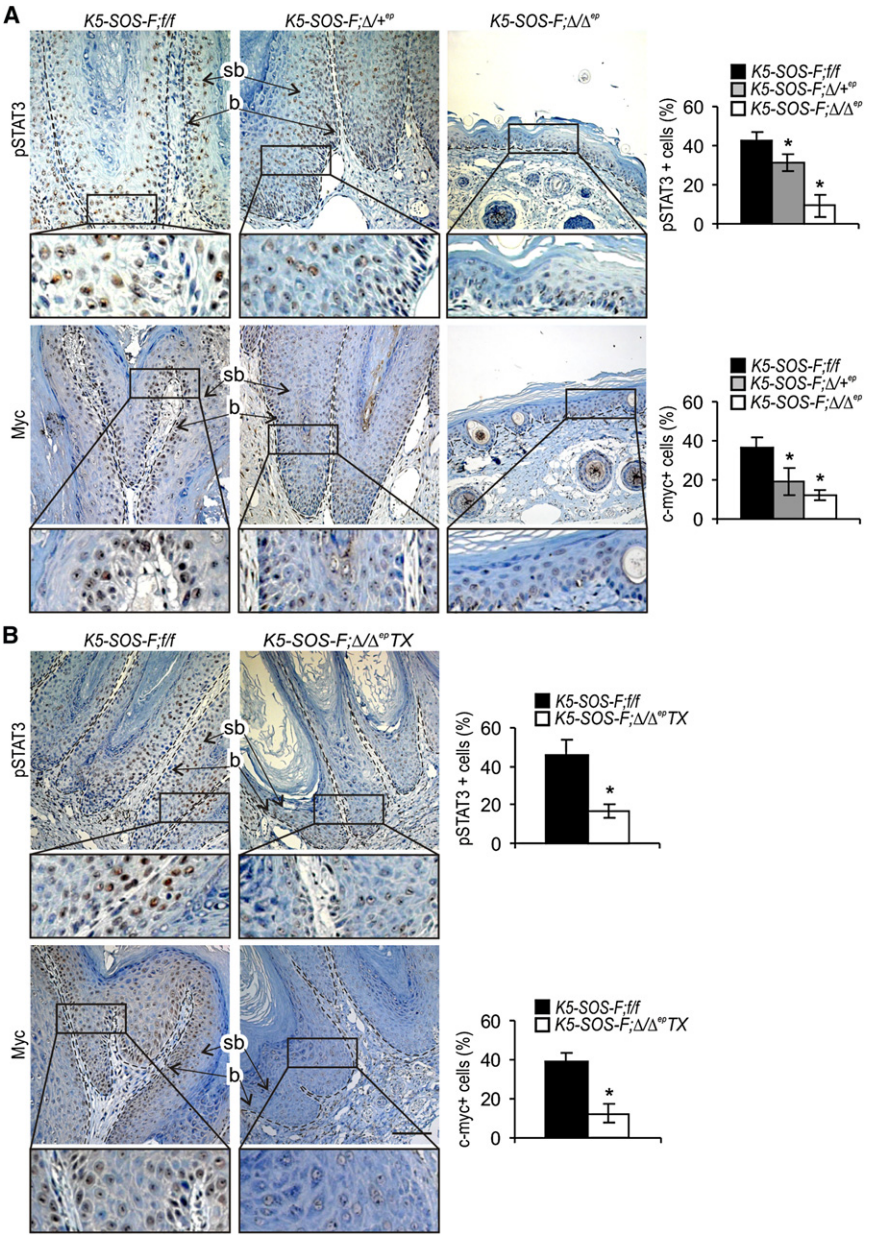

Figure 6. Chronic and Acute Raf-1 Ablation Decreases the Phosphorylation of STAT3 and the Expression of Myc in *K5-SOS-F* Tumors

(A) Raf-1 ablation decreases the phosphorylation of STAT3 (upper panel) and the expression of the STAT3 target Myc (lower panel) in *K5-SOS-F;Δ/+^{ep}* versus *K5-SOS-F;f/f* tumors. *K5-SOS-F;Δ/Δ^{ep}* epidermis is indistinguishable from epidermis not expressing the *K5-SOS-F* transgene. The scale bar represents 100 μm.

(B) STAT3 phosphorylation (upper panel) and Myc expression (lower panel) are dramatically reduced in regressing *K5-SOS-F;Δ/Δ^{ep}TX* tumors (day 7 after tamoxifen treatment). STAT3 phosphorylation and Myc expression were determined by immunohistochemistry of skin and tumor sections of the different genotypes as indicated. Positive cells are stained in brown. The scale bar represents 100 μm. The plots represent the results of the analysis of at least three animals/genotype, evaluating ≥600 cells/mouse. Error bars indicate SD of the mean. *$p < 0.01$ according to Student's t tests.

could not be easily quantified and taken into account in the plot (Figure 7C), which therefore understates the contribution of Rok to cofilin phosphorylation in vivo. Both STAT3 phosphorylation and Myc expression were strongly increased in the inhibitor-treated epidermis (Figures 7D and 7E), indicating that the cofilin/STAT3/Myc pathway is inhibited by Rok during the dedifferentiation of the keratinocytes required for tumor development. The *Δ/Δ^{ep}* animals were more resistant to the Rok inhibitor than the *Δ/+^{ep}* mice and had to be treated for a longer time period (6 weeks instead of 2) to achieve similar results. This is consistent with the idea that in *Δ/+^{ep}* epidermis the residual inhibition of Rok by Raf-1 synergizes with Y-27632 to allow dedifferentiation/proliferation, whereas the complete absence of Raf-1 in the *Δ/Δ^{ep}* epidermis renders it less permissive to the action of the inhibitor.

Together, the data link Raf-1 ablation with the activation of Rok, the inhibition of the cofilin/STAT3/Myc pathway, and the increased differentiation of Ras-induced tumors in vivo (Figure 7F).

DISCUSSION

The data above prove that in the mouse Raf-1 is required for the establishment and maintenance of skin tumors driven by the activation of Ras, achieved either by somatic mutation (DMBA/TPA model) or, more similar to the situation in human SCC, by the constitutive activation of the endogenous Ras pathway. Raf-1 ablation completely precludes tumor formation in both models and Raf-1 heterozygosity reduces it. More importantly, Raf-1 ablation causes the complete regression of established tumors. In contrast to the results obtained by interfering with other Ras effectors (Gonzalez-Garcia et al., 2005; Gupta et al., 2007; Malliri et al., 2002), the requirement for Raf-1 in Ras-driven carcinogenesis is absolute and it extends to tumor maintenance.

Raf-1 is also the first Ras effector for which a cell-autonomous requirement has been clearly demonstrated by the concomitant activation of Ras and ablation of Raf-1 in the same cell, the K5+ keratinocyte, in the context of an otherwise intact host. This does not, per se, rule out the possibility that a defective interaction of the Raf-1-deficient tumor cells with the stroma may contribute to the block of tumor development and maintenance, as we have recently described for B-Raf-deficient insulinomas (Sobczak et al., 2008). Such defects, however, could not explain the lack of primary tumor development observed in the *Δ/Δ^{ep}* epidermis

or the precipitous differentiation that follows Raf-1 ablation in established tumors. This accelerated differentiation can also be observed in cultured Raf-1-deficient keratinocytes, confirming the cell-autonomous nature of the defect (Figure 4).

In contrast to other Ras downstream targets such as RalGDS or PI-3K, whose main role is to support cell survival (Gonzalez-Garcia et al., 2005; Gupta et al., 2007), Raf-1 promotes tumor development by blocking differentiation. Surprisingly, this block in differentiation does not correlate with changes in the best-studied Raf downstream pathway MEK/ERK, whose activation was unchanged in Δ/Δ^{ep} epidermis and cultured keratinocytes. Instead, the Raf-1-dependent, SOS-F-induced differentiation block correlates with the reduced activation of Rok downstream targets, both in vivo in tumors and in keratinocytes differentiating in culture (Figures 4–6). In vivo treatment with a chemical Rok inhibitor induced dedifferentiation and increased proliferation in *K5-SOS-F;*Δ/Δ^{ep} epidermis (Figure 7), establishing a causal relationship between Rok inhibition by Raf-1 and the SOS-F-induced differentiation block. Rok inhibition reduced cofilin phosphorylation and increased STAT3 phosphorylation and Myc expression. Activation of the cofilin/STAT3/Myc pathway had been previously reported in hyperproliferating psoriatic epidermis, in which it blocks cell compaction (Honma et al., 2006), but it had never been implicated in tumorigenesis. Our data show that activation of this pathway correlates with a block in keratinocyte differentiation and increased proliferation in Ras-induced tumors in vivo, but we do not interpret them to mean that the inhibition of the cofilin/STAT3/Myc pathway is the only relevant event downstream of Rok in epidermal carcinogenesis; other targets of Rok not tested here, like the transcription factor NF-κB, may be equally relevant in this context (Dajee et al., 2003; van Hogerlinden et al., 1999).

Together, the data support the hypothesis that Raf-1 is deployed by activated Ras to counteract the activity of Rok by direct binding as previously reported (Ehrenreiter et al., 2005). Consistent with this theory, the interaction between Raf-1 and Rok-α was increased, and Rok-α activity decreased, in the *K5-SOS-F+* epidermis. Thus, one of the crucial functions of activated Ras in tumorigenesis is to prevent keratinocyte differentiation by restraining Rok activity, and Raf-1 is essential in this process (Figure 7F).

A role of Rok in cell differentiation and in the determination of cell fate has been recently emerging in other systems. Rok inhibition promotes the survival of human dissociated stem cells (Watanabe et al., 2007), perturbs epidermal stratification (Vaezi et al., 2002), and counteracts keratinocyte differentiation (Figures 4B and 7B; Honma et al., 2006; McMullan et al., 2003), whereas active Rok-α promotes it (McMullan et al., 2003). These observations are in line with a negative effect of Rok activation on tumorigenesis. In contrast, Rok is often upregulated in tumors (Sahai, 2005) and its activation can promote proliferation, invasion, and angiogenesis in xenograft models using human tumor cells (Croft et al., 2004; Itoh et al., 1999; Lefort et al., 2007). It is possible that the role of Rok in tumorigenesis is highly context dependent and that Rok activation may promote tumorigenesis when combined with mutations other than Ras activation. Alternatively, oncogenes are known to induce opposing signals, such as mitogenic and antiproliferative stress responses, the best known of which is senescence. Indeed, some of the genes synergistically upregulated by the combination of mutant p53 and Ras proteins in tumor cell lines have recently been proven antitumorigenic (McMurray et al., 2008). It is conceivable that the Rok overexpression observed in tumors may have originally been part of such an antiproliferative program. Be that as it may, the fact that Rok inhibition allows dedifferentiation and proliferation of *SOS-F+* epidermis, even in the absence of Raf-1, sounds a note of caution for the use of Rok inhibitors in the treatment of tumors, particularly of those relying on Ras activation.

Ras-driven skin tumors are addicted to Raf-1 in its role of endogenous Rok inhibitor, whereas Raf-1 signaling is not essential for epidermal development and homeostasis (Ehrenreiter et al., 2005). This discovery paves the way for the design of molecule-targeted therapies, which may include Raf-1 interference or allosteric inhibitors capable of disrupting the Raf-1:Rok complex. The treatment of cancer by inducing tumor cell differentiation in combination with chemotherapy has revolutionized the treatment of leukemia (Wang and Chen, 2008), but solid tumors have so far proven resistant. The complete differentiation induced by Raf-1 ablation in vivo raises hopes that combinations of Raf-1-targeted and conventional therapies may be successful at least in the treatment of Ras-driven skin epidermis tumors.

EXPERIMENTAL PROCEDURES

Mouse Strains, Genotyping, and Tumor Models

c-raf-1 Δ/Δ^{ep} or $\Delta/+^{ep}$, *K5-SOS-F*, and *K5-Cre-er(T)* mice and the respective genotyping have been described (Ehrenreiter et al., 2005; Indra et al., 1999; Sibilia et al., 2000). All strains were maintained on a 129Sv background. For chemical two-stage carcinogenesis, mice were shaved 3 days before initiation with DMBA (25 μg/200μl acetone; Sigma) applied to the dorsal skin. Beginning 3 days later, TPA (6 μg/100μl acetone; Sigma) was applied twice per week for 20 weeks. Control mice were treated with acetone (Hsieh et al., 2006). Onset, number, and size of tumors were monitored at least twice a week. Tumors developing in Δ/Δ^{ep} mice or relapsing after TX treatment were genotyped isolating the DNA from paraffin section and extending the *c-raf-1* PCR protocol by ten additional cycles to increase amplification. All animal experiments were performed in accordance with a protocol authorized by the Austrian Ministry of Science and Communications, following the approval by the national Ethical Committee for Animal Experimentation.

Histological Analysis

Hematoxylin/eosin staining and immunohistochemistry were performed on 3-μm-thick sections of 4% paraformaldehyde-fixed and paraffin-embedded tissues. Tail sections were decalcified by incubation of trimmed paraffin blocks for 10–15 min on paper towels soaked in 1 N HCl. Staining with the following antibodies was performed: α-BrdU (1:100; Zymed); α-c-*myc* (1:250; Milipore); α-E-cadherin (1:150; Santa Cruz); α-integrin β1 (1:50; BD Biosciences); α-K10 (1:500; BabCo); α-Ki67 (1:1000; Novocastra); α-pCofilin (Ser3, 1:50; Santa Cruz); α-pERK (Thr202/Tyr204, 1:50; Cell Signaling); and α-pSTAT3 (Tyr705, 1:100; Cell Signaling). For detection, we used the DAKO EnVision peroxidase system, followed by incubation with 0.01% diaminobenzidine (Sigma), in conjunction with avidin-biotinylated enzyme complex (Vector Laboratories) for biotinylated antibodies. Sections were counterstained with hematoxylin. BrdU incorporation was determined in mice injected with BrdU (12.5 mg/g body weight) 1 hr prior to tissue isolation.

Keratinocyte Isolation and Culture

Primary mouse keratinocytes were isolated from 18- to 21-day-old mice as previously described (Sibilia et al., 2000), plated at a density of ~6×10^6 cells/100 mm plate, and cultured in MEM (Sigma) containing 1 μg/ml insulin (Sigma), 5 ng/ml EGF (Roche), 5 μg/ml transferrin (Sigma), 10 μM phosphoethanolamine (Sigma), 10 μM ethanolamine (Sigma), 0.36 μg/ml hydrocortisone

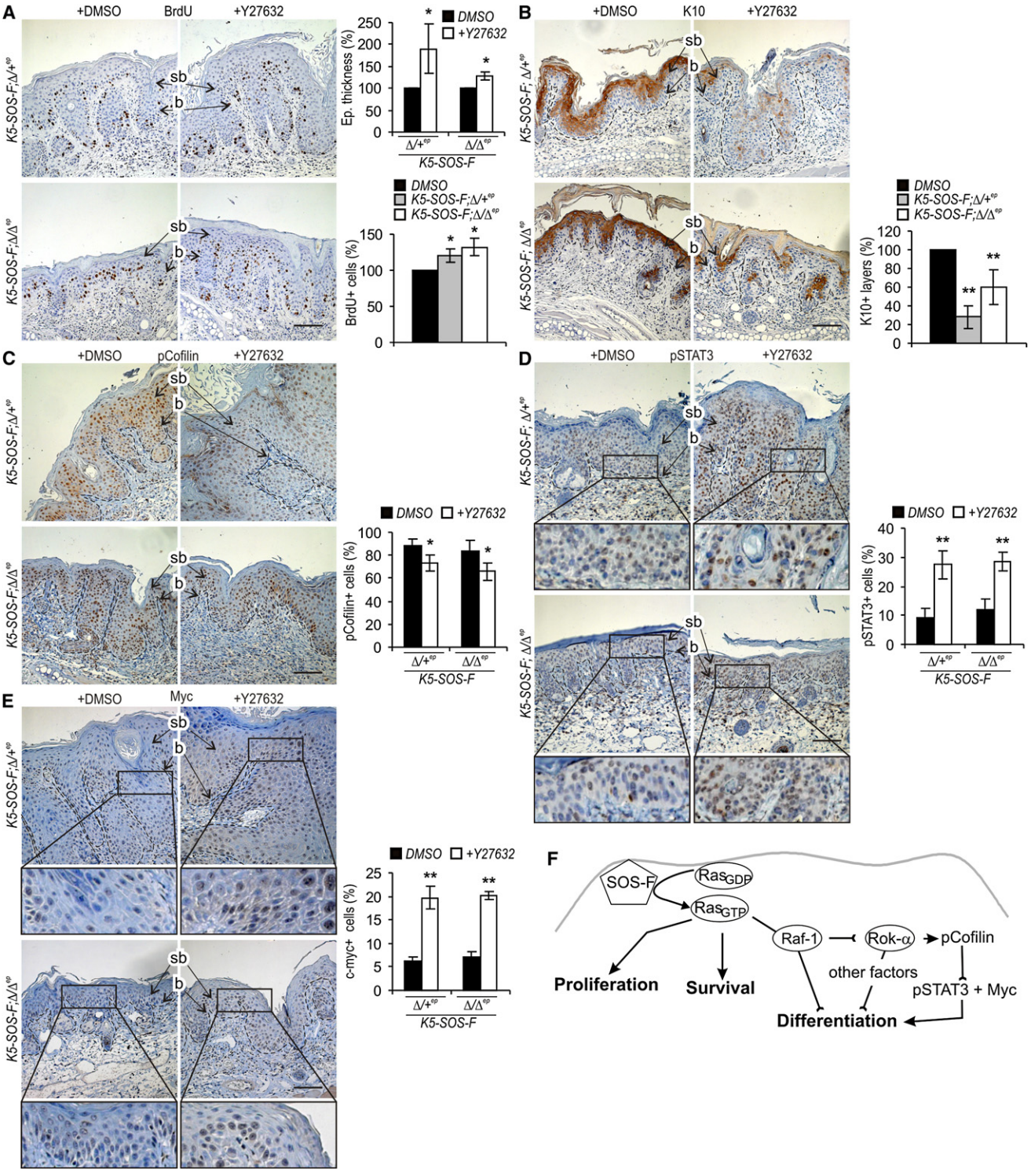

Figure 7. A Rok Inhibitor Induces Proliferation, Dedifferentiation, and Activation of the Cofilin/STAT3/Myc Pathway in the Epidermis of *K5-SOS-F;Δ/+ep* and *K5-SOS-F;Δ/Δep* Mice

Mice were treated with DMSO as a vehicle (left ear) or with Y-27632 (40 μM in DMSO; right ear) twice a day for 2 (*K5-SOS-F;Δ/+ep*) or 6 weeks (*K5-SOS-F;Δ/Δep*).

(A) Y-27632 causes proliferation of *K5-SOS-F;Δ/+ep* and *K5-SOS-F;Δ/Δep* epidermis. Proliferation was assessed both by counting the numbers of BrdU+ cells and by measuring epidermal thickness.

(B) Y-27632 causes dedifferentiation of *K5-SOS-F;Δ/+ep* and *K5-SOS-F;Δ/Δep* epidermis. Differentiation was assessed as the number of K10+ epidermal layers. In (A) and (B), proliferation and differentiation are expressed as a percentage of DMSO controls.

(Calbiochem), glutamine (Glutamax-I; Invitrogen), Pen/Strep (Invitrogen), and 6% chelated FCS (Chelex 100 Resin; Bio-Rad). The culture medium was exchanged every second day. For inducing differentiation, cells were transferred into starvation medium (containing only 2% chelated FCS and no growth factors) and treated with 1.2 mM $CaCl_2$ for different time periods. The Rok-α inhibitor Y-27632 (Calbiochem) and the MEK inhibitor U0126 (Cell Signaling) were added to the medium at a final concentration of 10 μM.

For the analysis of differentiation, cells were fixed in 4% PFA, permeabilized (0.2% Triton X-100), and blocked with 1% BSA before incubation with primary antibodies (α-Involucrin, 1:500; BabCo) followed by detection with the secondary FITC antibody (α-rabbit alexa 448 nm, 1:1500; Molecular Probes) and mounted with ProLong Antifade (Promega). Microscopical analysis was performed with an Axiovert 200 (Carl Zeiss MicroImaging, Inc.) equipped with an AxioCam. Images were acquired with the AxioVision Software (Carl Zeiss MicroImaging, Inc.) Proliferation was assessed by the In Situ Cell Proliferation Kit FLUOS (Roche) according to the manufacturer's recommendation. Cells were examined by light microscopy (Zeiss AxioVision; Carl Zeiss MicroImaging, Inc.), and the number of BrdU+ cells was quantified with the AutoMeasure software (Carl Zeiss MicroImaging, Inc.).

Rok-α Immunoprecipitation and Immunoprecipitation Kinase Assays

Crude epidermis lysates were prepared from the tail of 17-day-old mice. In brief, the skin was digested with trypsin to separate the epidermis from the dermis. The epidermis was placed in lysis buffer (200 mM Tris-HCl [pH 7.4], 2 mM EDTA, and 1% Triton X-100, supplemented with protease and phosphatase inhibitors) and homogenized with the PreCellys24 homogenizer (PeqLab). Rok-α immunoprecipitates were prepared from 1200 μg of protein with a Rok-α antibody (Upstate) and analyzed by immunoblotting or assayed for Rok-α kinase activity with the long S6 kinase (Upstate) as a substrate according to the manufacturer's instructions. The Rho kinase inhibitor Y-27632 (20 μM final) was used for assessment of Rok-α-specific kinase activity.

Immunoblotting

Membranes were probed with α-Cofilin (Abcam); α-panERK, α-Raf-1, α-Rok-α (Transduction Labs); α-panRasV12 (Calbiochem); α-pCofilin, α-pMLC2 (Santa Cruz); α-pERK (Cell Signaling); and α-SOS (BD Biosciences). After incubation with the appropriate secondary antibody, the antigens were visualized by ECL (Pierce).

Statistical Analysis

All values are expressed as mean (±SD) of at least three independent experiments. p values were calculated with the two-tailed Student's t test. A p value ≤ 0.05 is considered statistically significant.

SUPPLEMENTAL DATA

Supplemental Data contain four figures and can be found with this article online at http://www.cell.com/cancer-cell/supplemental/S1535-6108(09)00183-4.

ACKNOWLEDGMENTS

We thank E.F. Wagner and T. Decker for helpful discussions and M. Hamerl and the animal house team for excellent technical help. The *K5-Cre-er(T)* mice were a kind gift of P. Chambon. This work was supported by European Commission grant LSH-CT-2003-506803 and by Austrian Research Fund grant P19530-B11 (to M.B.).

Received: November 1, 2008
Revised: March 19, 2009
Accepted: June 10, 2009
Published: August 3, 2009

REFERENCES

Bailleul, B., Surani, M.A., White, S., Barton, S.C., Brown, K., Blessing, M., Jorcano, J., and Balmain, A. (1990). Skin hyperkeratosis and papilloma formation in transgenic mice expressing a ras oncogene from a suprabasal keratin promoter. Cell *62*, 697–708.

Benitah, S.A., Frye, M., Glogauer, M., and Watt, F.M. (2005). Stem cell depletion through epidermal deletion of Rac1. Science *309*, 933–935.

Chan, K.S., Sano, S., Kiguchi, K., Anders, J., Komazawa, N., Takeda, J., and DiGiovanni, J. (2004). Disruption of Stat3 reveals a critical role in both the initiation and the promotion stages of epithelial carcinogenesis. J. Clin. Invest. *114*, 720–728.

Chan, K.S., Sano, S., Kataoka, K., Abel, E., Carbajal, S., Beltran, L., Clifford, J., Peavey, M., Shen, J., and DiGiovanni, J. (2007). Forced expression of a constitutively active form of Stat3 in mouse epidermis enhances malignant progression of skin tumors induced by two-stage carcinogenesis. Oncogene *27*, 1087–1094.

Chen, S.-Y., Takeuchi, S., Moroi, Y., Hayashida, S., Kido, M., Chen, S.-J., Tomoeda, H., Uenotsuchi, T., Tu, Y.-T., Furue, M., et al. (2008). Overexpression of phosphorylated-ATF2 and STAT3 in cutaneous squamous cell carcinoma, Bowen's disease and basal cell carcinoma. J. Dermatol. Sci. *51*, 210–215.

Collado, M., Gil, J., Efeyan, A., Guerra, C., Schuhmacher, A.J., Barradas, M., Benguria, A., Zaballos, A., Flores, J.M., Barbacid, M., et al. (2005). Tumour biology: senescence in premalignant tumours. Nature *436*, 642.

Croft, D.R., Sahai, E., Mavria, G., Li, S., Tsai, J., Lee, W.M., Marshall, C.J., and Olson, M.F. (2004). Conditional ROCK activation in vivo induces tumor cell dissemination and angiogenesis. Cancer Res. *64*, 8994–9001.

Dajee, M., Tarutani, M., Deng, H., Cai, T., and Khavari, P.A. (2002). Epidermal Ras blockade demonstrates spatially localized Ras promotion of proliferation and inhibition of differentiation. Oncogene *21*, 1527–1538.

Dajee, M., Lazarov, M., Zhang, J.Y., Cai, T., Green, C.L., Russell, A.J., Marinkovich, M.P., Tao, S., Lin, Q., Kubo, Y., et al. (2003). NF-kappaB blockade and oncogenic Ras trigger invasive human epidermal neoplasia. Nature *421*, 639–643.

Ehrenreiter, K., Piazzolla, D., Velamoor, V., Sobczak, I., Small, J.V., Takeda, J., Leung, T., and Baccarini, M. (2005). Raf-1 regulates Rho signaling and cell migration. J. Cell Biol. *168*, 955–964.

Gonzalez-Garcia, A., Pritchard, C.A., Paterson, H.F., Mavria, G., Stamp, G., and Marshall, C.J. (2005). RalGDS is required for tumor formation in a model of skin carcinogenesis. Cancer Cell *7*, 219–226.

Green, C.L., and Khavari, P.A. (2004). Targets for molecular therapy of skin cancer. Semin. Cancer Biol. *14*, 63–69.

Grossi, M., Hiou-Feige, A., Tommasi Di Vignano, A., Calautti, E., Ostano, P., Lee, S., Chiorino, G., and Dotto, G.P. (2005). Negative control of keratinocyte differentiation by Rho/CRIK signaling coupled with up-regulation of KyoT1/2 (FHL1) expression. Proc. Natl. Acad. Sci. USA *102*, 11313–11318.

Gupta, S., Ramjaun, A.R., Haiko, P., Wang, Y., Warne, P.H., Nicke, B., Nye, E., Stamp, G., Alitalo, K., and Downward, J. (2007). Binding of ras to

(C) Y-27632 reduces cofilin phosphorylation in *K5-SOS-F;Δ/+^{ep}* and *K5-SOS-F;Δ/Δ^{ep}* epidermis. Both the number of pCofilin+ cells and the intensity of the staining are reduced. Only the first parameter, however, can be reliably quantified and is represented by the plot on the right, which therefore understates the result. (D and E) Y-27632 increases STAT3 phosphorylation (D) and Myc expression (E) in *K5-SOS-F;Δ/+^{ep}* and *K5-SOS-F;Δ/Δ^{ep}* epidermis. The plots in (C)–(E) show the percentage of positive cells in DMSO- versus Y-27632-treated epidermis. Positive cells are stained in brown. The scale bar represents 100 μm. The plots represent the results of the analysis of at least three animals/genotype, evaluating ≥600 cells/mouse. Error bars indicate SD of the mean. *$p < 0.05$ and **$p < 0.01$ according to Student's t tests.

(F) Role of Raf-1 in SOS-F-driven tumorigenesis. Our data are consistent with a working model in which Raf-1 is essential to inhibit Rok-α activity. Rok-α activates downstream pathways, including the phosphorylation of cofilin and a decrease in STAT3 phosphorylation and Myc expression, which induce keratinocyte differentiation.

phosphoinositide 3-kinase p110alpha is required for ras-driven tumorigenesis in mice. Cell *129*, 957–968.

Haase, I., Hobbs, R.M., Romero, M.R., Broad, S., and Watt, F.M. (2001). A role for mitogen-activated protein kinase activation by integrins in the pathogenesis of psoriasis. J. Clin. Invest. *108*, 527–536.

Honma, M., Benitah, S.A., and Watt, F.M. (2006). Role of LIM kinases in normal and psoriatic human epidermis. Mol. Biol. Cell *17*, 1888–1896.

Hsieh, Y.H., Juliana, M.M., Hicks, P.H., Feng, G., Elmets, C., Liaw, L., and Chang, P.L. (2006). Papilloma development is delayed in osteopontin-null mice: implicating an antiapoptosis role for osteopontin. Cancer Res. *66*, 7119–7127.

Indra, A.K., Warot, X., Brocard, J., Bornert, J.M., Xiao, J.H., Chambon, P., and Metzger, D. (1999). Temporally-controlled site-specific mutagenesis in the basal layer of the epidermis: comparison of the recombinase activity of the tamoxifen-inducible Cre-ER(T) and Cre-ER(T2) recombinases. Nucleic Acids Res. *27*, 4324–4327.

Ise, K., Nakamura, K., Nakao, K., Shimizu, S., Harada, H., Ichise, T., Miyoshi, J., Gondo, Y., Ishikawa, T., Aiba, A., et al. (2000). Targeted deletion of the H-ras gene decreases tumor formation in mouse skin carcinogenesis. Oncogene *19*, 2951–2956.

Itoh, K., Yoshioka, K., Akedo, H., Uehata, M., Ishizaki, T., and Narumiya, S. (1999). An essential part for Rho-associated kinase in the transcellular invasion of tumor cells. Nat. Med. *5*, 221–225.

Lashmar, U.T., Hadgraft, J., and Thomas, N. (1989). Topical application of penetration enhancers to the skin of nude mice: a histopathological study. J. Pharm. Pharmacol. *41*, 118–122.

Lefort, K., Mandinova, A., Ostano, P., Kolev, V., Calpini, V., Kolfschoten, I., Devgan, V., Lieb, J., Raffoul, W., Hohl, D., et al. (2007). Notch1 is a p53 target gene involved in human keratinocyte tumor suppression through negative regulation of ROCK1/2 and MRCKalpha kinases. Genes Dev. *21*, 562–577.

Leicht, D.T., Balan, V., Kaplun, A., Singh-Gupta, V., Kaplun, L., Dobson, M., and Tzivion, G. (2007). Raf kinases: Function, regulation and role in human cancer. Biochim. Biophys. Acta *1773*, 1196–1212.

Levy, L., Broad, S., Diekmann, D., Evans, R.D., and Watt, F.M. (2000). beta1 integrins regulate keratinocyte adhesion and differentiation by distinct mechanisms. Mol. Biol. Cell *11*, 453–466.

Lim, K.-H., and Counter, C.M. (2005). Reduction in the requirement of oncogenic Ras signaling to activation of PI3K/AKT pathway during tumor maintenance. Cancer Cell *8*, 381–392.

Lin, A.W., and Lowe, S.W. (2001). Oncogenic ras activates the ARF-p53 pathway to suppress epithelial cell transformation. Proc. Natl. Acad. Sci. USA *98*, 5025–5030.

Malliri, A., van der Kammen, R.A., Clark, K., van der Valk, M., Michiels, F., and Collard, J.G. (2002). Mice deficient in the Rac activator Tiam1 are resistant to Ras-induced skin tumours. Nature *417*, 867–871.

Mavria, G., Vercoulen, Y., Yeo, M., Paterson, H., Karasarides, M., Marais, R., Bird, D., and Marshall, C.J. (2006). ERK-MAPK signaling opposes Rho-kinase to promote endothelial cell survival and sprouting during angiogenesis. Cancer Cell *9*, 33–44.

McMullan, R., Lax, S., Robertson, V.H., Radford, D.J., Broad, S., Watt, F.M., Rowles, A., Croft, D.R., Olson, M.F., and Hotchin, N.A. (2003). Keratinocyte differentiation is regulated by the Rho and ROCK signaling pathway. Curr. Biol. *13*, 2185–2189.

McMurray, H.R., Sampson, E.R., Compitello, G., Kinsey, C., Newman, L., Smith, B., Chen, S.-R., Klebanov, L., Salzman, P., Yakovlev, A., et al. (2008). Synergistic response to oncogenic mutations defines gene class critical to cancer phenotype. Nature *453*, 1112–1116.

Mueller, M.M. (2006). Inflammation in epithelial skin tumours: Old stories and new ideas. Eur. J. Cancer *42*, 735–744.

Porter, R.M., Reichelt, J., Lunny, D.P., Magin, T.M., and Lane, E.B. (1998). The relationship between hyperproliferation and epidermal thickening in a mouse model for BCIE. J. Invest. Dermatol. *110*, 951–957.

Quintanilla, M., Brown, K., Ramsden, M., and Balmain, A. (1986). Carcinogen-specific mutation and amplification of Ha-ras during mouse skin carcinogenesis. Nature *322*, 78–80.

Repasky, G.A., Chenette, E.J., and Der, C.J. (2004). Renewing the conspiracy theory debate: does Raf function alone to mediate Ras oncogenesis? Trends Cell Biol. *14*, 639–647.

Ridky, T.W., and Khavari, P.A. (2004). Pathways sufficient to induce epidermal carcinogenesis. Cell Cycle *3*, 621–624.

Riva, C., Lavieille, J.P., Reyt, E., Brambilla, E., Lunardi, J., and Brambilla, C. (1995). Differential c-myc, c-jun, c-raf and p53 expression in squamous cell carcinoma of the head and neck: Implication in drug and radioresistance. Eur. J. Cancer B Oral Oncol. *31B*, 384–391.

Roper, E., Weinberg, W., Watt, F.M., and Land, H. (2001). p19ARF-independent induction of p53 and cell cycle arrest by Raf in murine keratinocytes. EMBO Rep. *2*, 145–150.

Sahai, E. (2005). Mechanisms of cancer cell invasion. Curr. Opin. Genet. Dev. *15*, 87–96.

Sano, S., Itami, S., Takeda, K., Tarutani, M., Yamaguchi, Y., Miura, H., Yoshikawa, K., Akira, S., and Takeda, J. (1999). Keratinocyte-specific ablation of stat3 exhibits impaired skin remodeling, but does not affect skin morphogenesis. EMBO J. *18*, 4657–4668.

Schmidt, M., Goebeler, M., Posern, G., Feller, S.M., Seitz, C.S., Brocker, E.-B., Rapp, U.R., and Ludwig, S. (2000). Ras-independent activation of the Raf/MEK/ERK pathway upon calcium-induced differentiation of keratinocytes. J. Biol. Chem. *275*, 41011–41017.

Scholl, F.A., Dumesic, P.A., and Khavari, P.A. (2004). Mek1 alters epidermal growth and differentiation. Cancer Res. *64*, 6035–6040.

Seethala, R.R., Gooding, W.E., Handler, P.N., Collins, B., Zhang, Q., Siegfried, J.M., and Grandis, J.R. (2008). Immunohistochemical analysis of phosphotyrosine signal transducer and activator of transcription 3 and epidermal growth factor receptor autocrine signaling pathways in head and neck cancers and metastatic lymph nodes. Clin. Cancer Res. *14*, 1303–1309.

Sibilia, M., Fleischmann, A., Behrens, A., Stingl, L., Carroll, J., Watt, F.M., Schlessinger, J., and Wagner, E.F. (2000). The EGF receptor provides an essential survival signal for SOS-dependent skin tumor development. Cell *102*, 211–220.

Sobczak, I., Galabova-Kovacs, G., Sadzak, I., Kren, A., Christofori, G., and Baccarini, M. (2008). B-Raf is required for ERK activation and tumor progression in a mouse model of pancreatic [beta]-cell carcinogenesis. Oncogene *27*, 4779–4787.

Solit, D.B., Garraway, L.A., Pratilas, C.A., Sawai, A., Getz, G., Basso, A., Ye, Q., Lobo, J.M., She, Y., Osman, I., et al. (2006). BRAF mutation predicts sensitivity to MEK inhibition. Nature *439*, 358–362.

Tarutani, M., Cai, T., Dajee, M., and Khavari, P.A. (2003). Inducible activation of Ras and Raf in adult epidermis. Cancer Res. *63*, 319–323.

Vaezi, A., Bauer, C., Vasioukhin, V., and Fuchs, E. (2002). Actin cable dynamics and Rho/Rock orchestrate a polarized cytoskeletal architecture in the early steps of assembling a stratified epithelium. Dev. Cell *3*, 367–381.

van Hogerlinden, M., Rozell, B.L., Ahrlund-Richter, L., and Toftgard, R. (1999). Squamous cell carcinomas and increased apoptosis in skin with inhibited Rel/nuclear factor-kappaB signaling. Cancer Res. *59*, 3299–3303.

Wakamatsu, K., Ogita, H., Okabe, N., Irie, K., Tanaka-Okamoto, M., Ishizaki, H., Ishida-Yamamoto, A., Iizuka, H., Miyoshi, J., and Takai, Y. (2007). Up-regulation of loricrin expression by cell adhesion molecule nectin-1 through Rap1-ERK signaling in keratinocytes. J. Biol. Chem. *282*, 18173–18181.

Wang, Z.Y., and Chen, Z. (2008). Acute promyelocytic leukemia: from highly fatal to highly curable. Blood *111*, 2505–2515.

Watanabe, K., Ueno, M., Kamiya, D., Nishiyama, A., Matsumura, M., Wataya, T., Takahashi, J.B., Nishikawa, S., Nishikawa, S.-i., Muguruma, K., et al. (2007). A ROCK inhibitor permits survival of dissociated human embryonic stem cells. Nat. Biotechnol. *25*, 681–686.

Watt, F.M., Frye, M., and Benitah, S.A. (2008). MYC in mammalian epidermis: how can an oncogene stimulate differentiation? Nat. Rev. Cancer *8*, 234–242.

Wu, X., Quondamatteo, F., Lefever, T., Czuchra, A., Meyer, H., Chrostek, A., Paus, R., Langbein, L., and Brakebusch, C. (2006). Cdc42 controls progenitor cell differentiation and beta-catenin turnover in skin. Genes Dev. *20*, 571–585.

Zhao, Z.S., and Manser, E. (2005). PAK and other Rho-associated kinases–effectors with surprisingly diverse mechanisms of regulation. Biochem. J. *386*, 201–214.